

ESR of Au:Yb thin films: Crystal-field effects and the Kondo dilemma

F. G. Gandra, C. A. Pelá, G. E. Barberis, D. Davidov,* and C. Rettori

Instituto de Física "Gleb Wataghin," Universidade Estadual de Campinas, 13100 Campinas, S.P., Brasil

(Received 11 September 1979)

ESR experiments at liquid-helium temperatures on Au:Yb thin films evaporated on quartz and NaCl substrates are reported. The anisotropy on the Γ_7 g value of the Yb resonance, caused by the planar strain, induced by the difference in thermal expansion coefficients between the film and substrate, enable us to estimate lower limits for the tetragonal and trigonal second-order orbit-lattice coupling parameters. The hydrostatic component of the deformation, which is of the order of 1%, has no effect on the g value. These results enable us to estimate an upper limit for the logarithmic volume derivative of the exchange parameter.

I. INTRODUCTION

The system Au:Yb has been extensively studied in the past ten years.¹⁻⁷ Early ESR studies¹ on bulk and powdered samples have indicated a negative g shift for the Yb³⁺ ions in Au which could be attributed to a negative covalent mixing type of exchange coupling between the Yb³⁺ ion and the conduction electrons. Later this negative exchange coupling was confirmed by the observation of a Kondo minimum in the resistivity,² as well as by the observation of Kondo-like relaxation in a Mössbauer experiment of Au:Yb.³ The Mössbauer study as analyzed by Gonzalez-Jimenez *et al.*⁴ yields a Kondo temperature T_K in the vicinity of $T_K \cong 1$ mK. In contrast to these experiments and interpretations, however, no evidence for a Kondo effect was observed in a recent magnetization measurement⁵ and a nuclear orientation study⁶ in the millikelvin temperature range, indicating that the Kondo temperature of Au:Yb is some tenths of a millikelvin or lower.

In order to shed more light on these discrepancies, we have carried out ESR measurement on Au:Yb thin films evaporated on quartz and NaCl substrates. Owing to the different contraction of both the metallic Au:Yb film and the substrate (NaCl, quartz) between the deposition temperature T_d and the measured temperature T_m , strains are induced in the Au:Yb thin film, both planar strains and uniform hydrostatic strains.⁸⁻¹² The induced planar strains at the interface (xy) plane can be calculated, knowing the thermal expansion coefficients $\alpha_{Au}(T)$ and $\alpha_{subs}(T)$ of Au and the substrate, respectively, as follows⁸

$$\epsilon_{xx} = \epsilon_{yy} = \int_{T_m}^{T_d} [\alpha_{Au}(T) - \alpha_{subs}(T)] dT, \quad (1)$$

whereas ϵ_{zz} can be obtained using Eq. (1) together with the elastic compliances constants S_{ij} for Au as

follows¹³:

$$\frac{\epsilon_{zz}}{\epsilon_{xx}} = \frac{2S_{12}}{S_{11} + S_{12}} = \alpha \quad (2a)$$

for the [001] oriented films and

$$\frac{\epsilon_{zz}}{\epsilon_{xx}} = \frac{2(S_{11} + 2S_{12} - S_{44})}{2S_{11} + 4S_{12} + S_{44}} = \beta \quad (2b)$$

for the [111] films.

Using Eqs. (1) and (2), the hydrostatic strain $\epsilon_{xx} + \epsilon_{yy} + \epsilon_{zz}$ can be estimated to be -1.17% and 1.03% in Au:Yb thin films grown on NaCl and quartz substrates, respectively.

In a Kondo system, such expansion and contraction (equivalent to external pressure of 50 kbar approximately) should change dramatically the g shift induced by the conduction electrons via the Yb³⁺ conduction-electron exchange coupling. This is because the exchange coupling in a Kondo system is dominated by a covalent mixing mechanism which depends on the energy splitting between the Fermi energy E_F and the $4f$ level E_7 . This energy splitting is very sensitive to external pressure or changes in the lattice constants. Indeed extensive studies under external pressure in a large class of Kondo systems^{14,15} has indicated dramatic changes in the Kondo temperature which could be attributed to shift of the Fermi energy with respect to the localized moment energy. In the case of Au:Yb, such an effect should be more pronounced, as Gonzalez-Jimenez *et al.*⁴ in their interpretation of the Au:Yb Mössbauer data have estimated a relatively small splitting (approximately 0.02 eV) between the Yb³⁺ Γ_7 ground state E_7 and the Fermi energy.

Our measurement has shown angular dependent g value and linewidth for Au:Yb thin films evaporated on NaCl single-crystal substrate. This angular variation is attributed to planar (uniaxial) strains and have

been observed already in other systems such as Ag:Er,^{8,10} Au:Er,^{9,12} and Ag:Dy.¹¹ The angular variation enabled one to estimate a lower limit for the orbit-lattice coupling parameters. Within the accuracy of our measurements, no evidence for a shift induced by the hydrostatic lattice expansion or contraction was observed. This might indicate that the energy splitting $E_7 - E_F$ is significantly larger than was assumed previously.⁴ Thus, our measurements would support very low Kondo condensation temperature for Au:Yb in agreement with the nuclear orientation⁶ and the magnetization measurements.⁵

II. EXPERIMENT AND RESULTS

Thin films of Au:Yb with thicknesses between 900 and 4500 Å were grown in an ultrahigh vacuum system (10^{-8} Torr), by the coevaporation method. Evaporation rates of 300 and 3.6 Å/sec for Au and Yb, respectively, were used in order to achieve concentrations of the order of 0.5 at. % at the film. The substrates were either amorphous quartz or NaCl (001)- and (111)-oriented single crystals. In order to achieve good epitaxial growth for the (001) and (111) single-crystal thin films, the NaCl (001) and (111) surfaces were obtained by cleaving and polishing in air the NaCl substrates, respectively. The surfaces were washed with water and heated up to about 400 °C for the (001)-oriented films and 350 °C for the (111)-oriented films during evaporation. At lower deposition temperatures, the films tend to naturally grow in the [111] direction, almost independent of the substrate, but with a mosaic structure,⁹ as x-ray-diffraction and electron-microscopy analyses have demonstrated. Also mosaic structure was found for films evaporated on hot quartz substrates. Deposition temperatures from 40 to 400 °C were used in order to study the g -value anisotropy as a function of the deformation. The films were kept in a dry argon atmosphere prior to the ESR experiment. It was found that those films which were exposed to air at room atmosphere lost the EPR signal completely after a few days.

The ESR experiments have been carried out at temperatures between 1.4 and 4.2 K, using a conventional Varian ESR spectrometer and a stainless-steel Dewar with a quartz tail, which fits into a 100 kHz TE_{102} Varian cavity and allows sample rotation.

Figure 1 shows a typical Yb spectra from a Au:Yb film of 4200 Å evaporated on a hot NaCl (001) substrate. The magnetic field lies at 55° from the direction perpendicular to the plane of the film. Figure 2 gives the angular variation of the g value and linewidth for two films evaporated on quartz and NaCl(111) substrates; the magnetic field is rotated on a plane perpendicular to the plane of the film. The solid lines are the best fits of the data to the follow-

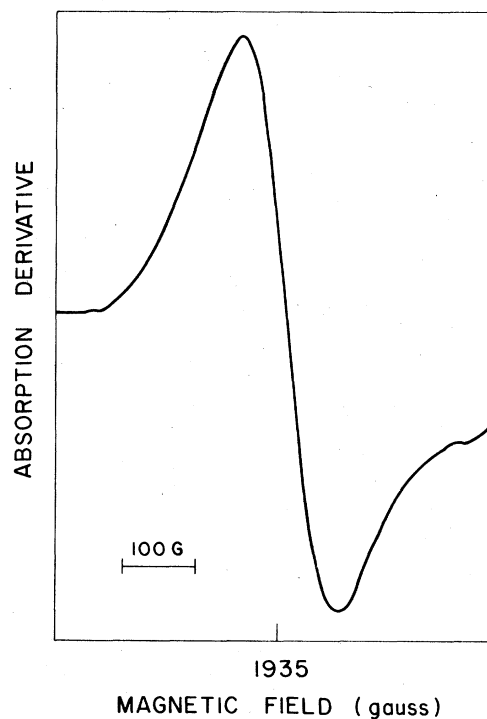


FIG. 1. ESR spectra at 1.4 K, of Au:Yb 4200-Å (001)-oriented thin film. The magnetic field is oriented at 55° from the direction perpendicular to the plane of the film.

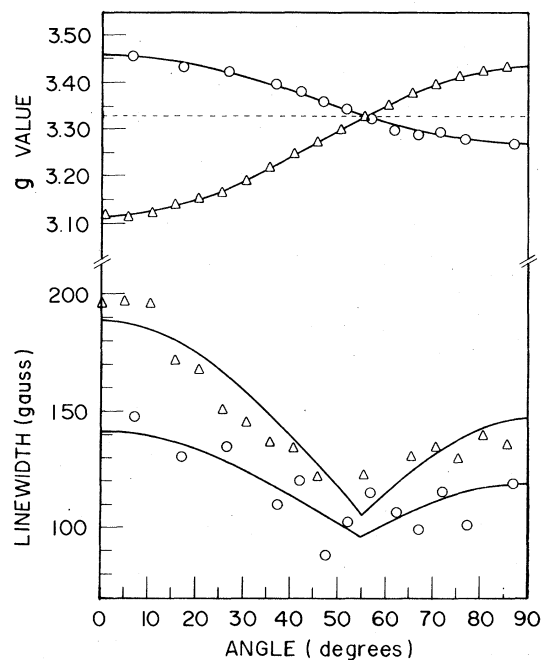


FIG. 2. Linewidth and g -value anisotropy at 1.4 K for two Au:Yb films when the magnetic field is rotated in a plane perpendicular to the plane of the film. Δ and \circ are the experimental points corresponding to films with 4300 Å of thicknesses deposited on quartz and NaCl(111), respectively.

ing expressions:

$$g = g_0 + \frac{1}{2} \Delta g (3 \cos^2 \Theta - 1) \quad (3)$$

and

$$\Delta H = \Delta H_0 + \frac{1}{2} \Delta H_1 |3 \cos^2 \Theta - 1|, \quad (4)$$

where g_0 , Δg , ΔH_0 , and ΔH_1 are the experimental parameters obtained from the fittings. Table I gives these parameters, for all the analyzed films. Table I contains, also, information about the film thicknesses, deposition temperatures, deformation (estimated from the difference in thermal expansion coefficients between the substrate and film),¹³ as well as the results of the x-ray analysis. The error bars in Table I were obtained from a statistical propagation of the experimental errors.

It should be stressed that, in the strain-free Au:Yb films (after the film was taken out from the substrate), we found the thermal broadening of the linewidth and the g value to be 35 ± 20 G/K and 3.33 ± 0.02 , respectively. These values agree with measurements on Au:Yb bulk and powdered samples.¹ In few cases where a good signal-to-noise ratio and narrow lines were observed, a hyperfine splitting of 575 ± 20 G was measured.¹ In most of the cases the resonance showed an almost symmetric line shape, characteristic of thicknesses comparable with the skin depth. The spectra have been analyzed by the method of Peter *et al.*¹⁶ No angular variation, ei-

ther in the g value or linewidth, was observed on the strain-free films, indicating that neither remanent strains nor random stresses were left on the films.

As in previous measurements on Au:Er thin films, the anisotropy of the g value for (001) single-crystal thin films is strongly dependent on the thickness of the film (see Table I). For films thicker than 900 Å this anisotropy drops drastically. We believe that this is due to a decrease in the deformation for thick films¹² which might be associated with sliding off the film from the substrate, or to a significant increase of the nonuniformity of the deformation across the film for thicker films. This, however, seems to be unlikely because the anisotropy of the linewidths does not increase significantly for thick films, as it should in the case of gross nonuniformity of the deformation across the film. Therefore we shall use films with thicknesses of 900 Å having maximum anisotropy of g value, to estimate a lower limit of the tetragonal second-order orbit-lattice coupling constant.

Again, as in the case of Au:Er,¹² the g -value anisotropy for (111)-oriented thin films, either single crystals or those with mosaic structure, depend strongly upon the type of substrate, of surface and thicknesses (see Table I), suggesting that sliding-off effects at the interface might also take place here. Therefore we shall use the maximum observed anisotropy per unit strain of the g value to estimate a lower limit for the trigonal second-order orbit-lattice coupling constant. This corresponds to films evaporated on quartz sub-

TABLE I. Experimental ESR data for Au:Yb thin films.

Substrate	Thickness ^a (Å)	Deposition temperature ^a (°C)	Deformation ϵ_{xx} (%)	g_0	Δg	ΔH_0 (G)	ΔH_1 (G)	Film structure (x ray)	$\xi =$ $\frac{(\Delta \epsilon^2(z))^{1/2}}{\langle \epsilon(z) \rangle}$
NaCl (001)	900	370	-1.72	3.32 ± 0.02	-0.030 ± 0.015	300 ± 100	<30	(001)	...
	4200	390	-1.80	3.32 ± 0.01	-0.020 ± 0.004	88 ± 20	<8	(001)	...
NaCl (001)	4300	60	-0.63	3.33 ± 0.03	0.090 ± 0.006	176 ± 30	<10	(111) ^b	...
	1000	350	-1.64	3.30 ± 0.04	0.040 ± 0.007	210 ± 40	<15	(111) ^b	...
NaCl (111)	1000	340	-1.53	3.34 ± 0.03	0.030 ± 0.009	204 ± 80	<30	(111)	...
	2100	360	-1.68	3.33 ± 0.02	0.160 ± 0.005	113 ± 20	<8	(111)	...
	4300	60	-0.63	3.33 ± 0.02	0.130 ± 0.005	97 ± 18	45	(111) ^b	0.59
	4500	200	-1.07	3.32 ± 0.02	0.040 ± 0.005	108 ± 20	<8	(111) ^b	...
	4300	207	-1.10	3.34 ± 0.02	0.110 ± 0.005	113 ± 22	45	(111) ^b	...
Quartz	4300	275	-1.35	3.33 ± 0.02	0.060 ± 0.006	138 ± 30	<10	(111) ^b	0.51
	4200	350	-1.64	3.32 ± 0.01	0.100 ± 0.005	88 ± 15	30	(111)	...
	1000	340	0.79	3.35 ± 0.04	-0.260 ± 0.015	250 ± 100	<30	(111) ^b	...
	4200	60	0.36	3.33 ± 0.01	-0.140 ± 0.004	82 ± 15	39	(111) ^b	0.48
Quartz	4300	287	0.72	3.32 ± 0.02	-0.290 ± 0.005	114 ± 22	93	(111) ^b	0.55
	4300	350	0.81	3.33 ± 0.02	-0.210 ± 0.005	107 ± 20	83	(111) ^b	0.67

^aThe thicknesses and deposition temperatures are determined within 10%.

^bMosaic structure.

strates (see Table I). Though the structure of these films is of the mosaic type, it was shown¹¹ that even in this case only one parameter (the trigonal one) enter into the analysis of the g -value anisotropy.

In the case of films evaporated on quartz substrates at different deposition temperatures the g -value anisotropy, almost scale with the expected deformation, which indicate that for these substrates the sliding-off effects might not be too important. But in any case we still can only estimate a lower limit for the parameters, since angular variations of the linewidths, characteristic of nonuniform stress distribution across the film, are always present in our films.

III. THEORETICAL CONSIDERATIONS

The theoretical considerations in analyzing ESR in metallic film epitaxially grown on a substrate have been discussed previously.⁸⁻¹² Here we shall apply some of the basic ideas to interpret our ESR measurements on Au:Yb films. As demonstrated previously,⁸⁻¹² a stress distribution across the film would lead to an angular dependent g value, that for a (001)-oriented film can be expressed, in the first approximation,⁸ as

$$g(\Theta) = g_0 + \frac{1}{2} g_{3g} \langle \epsilon_{3g\Theta}(z) \rangle (3 \cos^2 \Theta - 1) , \quad (5)$$

while for (111)-oriented film one finds⁹

$$g(\Theta) = g_0 + \frac{1}{2} g_{5g} \langle \epsilon_{5g}(z) \rangle (3 \cos^2 \Theta - 1) , \quad (6)$$

where $\langle \epsilon_{3g\Theta}(z) \rangle$ and $\langle \epsilon_{5g}(z) \rangle$ are the mean values of the normal strains $\epsilon_{3g\Theta}$ and ϵ_{5g} across the film. The values of the normal strains at the interface are given by

$$\epsilon_{3g\Theta} = (\alpha - 1) \epsilon_{xx} \quad (7)$$

for the (001) films and

$$\epsilon_{5g} = (\sqrt{3}/3)(\beta - 1) \epsilon_{xx} \quad (8)$$

for the (111) films. The strain components ϵ_{ij} , α , and β are defined by Eqs. (1) and (2). For uniform strains we expect $|\langle \epsilon_{3g\Theta}(z) \rangle| = |\epsilon_{3g\Theta}(z)|$ and $|\langle \epsilon_{5g}(z) \rangle| = |\epsilon_{5g}(z)|$; for nonuniform strains ϵ_{5g} and $\epsilon_{3g\Theta}$ represents upper limits for $\langle \epsilon_{3g\Theta}(z) \rangle$ and $\langle \epsilon_{5g}(z) \rangle$. The coefficients g_{3g} and g_{5g} are related to the orbit-lattice coupling parameters $G_{3g}^{(2)}$ and $G_{5g}^{(2)}$

(defined by the orbit-lattice Hamiltonian, see Ref. 8) as follows¹⁷:

$$g_{3g} = g(\Gamma_7) \frac{G_{3g}^{(2)}}{E_7 - E_8} \times \frac{\langle \Gamma_{7\alpha} | J_z | \Gamma_{8\mu} \rangle \langle \Gamma_{8\mu} | 3J_z^2 - J(J+1) | \Gamma_{7\alpha} \rangle}{\langle \Gamma_{7\alpha} | J_z | \Gamma_{7\alpha} \rangle} \quad (9)$$

and

$$g_{5g} = \frac{3}{4} g(\Gamma_7) \frac{G_{5g}^{(2)}}{E_7 - E_8} \times \frac{\langle \Gamma_{7\beta} | J_+ | \Gamma_{8\lambda} \rangle \langle \Gamma_{8\lambda} | J_+^2 - J_-^2 | \Gamma_{7\beta} \rangle}{\langle \Gamma_{7\alpha} | J_z | \Gamma_{7\alpha} \rangle} , \quad (10)$$

where we have taken into consideration the admixture of the Γ_7 ground state and the Γ_8 excited state but have neglected terms with $l=4, 6$ because they are expected to be at least, one order of magnitude smaller than the $l=2$ contributions.⁸

Any hydrostatic part of the strain field should manifest itself in the value of g_0 [Eqs. (3) and (4)]. g_0 represents the sum of the ionic g value g_{ion} and the g shift induced by the conduction electrons Δg_{ce} , which can be expressed as

$$\Delta g_{ce} = g(\Gamma_7) (g_J - 1) / g_J J \eta(E_F) , \quad (11)$$

where g_J is the Yb³⁺ Landé g factor, J is the exchange coupling between the Yb ion and the conduction electrons, and $\eta(E_F)$ is the density of states of the conduction electrons at the Fermi level. Consequently we expect, assuming the free-electron model for the density of state, that any volume modification of either the exchange parameter J or the Fermi energy E_F would induce a change in the g shift given by

$$\frac{\delta(\Delta g_{ce})}{\Delta g_{ce}} = \frac{\delta V}{V} \frac{\partial(\ln J)}{\partial(\ln V)} - \frac{\partial(\ln E_F)}{\partial(\ln V)} , \quad (12)$$

where the second term on the right can be estimated theoretically¹⁵ in the frame of the free-electron model to be $-\frac{2}{3}$.

We turn now to discuss the angular dependence of the linewidth. In the case of uniform stress distribution across the film, no angular dependence is expected. However, for nonuniform stress the linewidth for the (001)-oriented film can be written as

$$\Delta H(\theta) = \Delta H_0 + \frac{1}{2} H_0 [g_{3g}/g(\Gamma_7)] \langle \Delta \epsilon_{3g\Theta}^2(z) \rangle^{1/2} |3 \cos^2 \theta - 1| , \quad (13)$$

while for the (111)-oriented film

$$\Delta H(\theta) = \Delta H_0 + \frac{1}{2} H_0 [g_{5g}/g(\Gamma_7)] \langle \Delta \epsilon_{5g}^2(z) \rangle^{1/2} |3 \cos^2 \theta - 1| . \quad (14)$$

Here $\langle \Delta \epsilon_{3g\theta}^2(z) \rangle^{1/2}$ and $\langle \Delta \epsilon_{5g}^2(z) \rangle^{1/2}$ represents the dispersion of the strains distribution along an axis perpendicular to the film plane. Consequently the value of $\langle \Delta \epsilon^2(z) \rangle^{1/2} / \langle \epsilon(z) \rangle$, gives one an idea about the nonuniformity of the strains across the film. Table I exhibit the parameter $\xi = \langle \Delta \epsilon^2(z) \rangle / \langle \epsilon(z) \rangle$ for some of the films studied.

IV. ANALYSIS AND DISCUSSION

The angular dependence of the experimental g value can be very well described by Eqs. (5) and (6). The solid line in Fig. 2 is the best fit of the theory to the experimental results. The fitting procedure yield a value for the two unknown parameters, namely, $g_{3g} \langle \epsilon_{3g\theta}(z) \rangle$ and g_0 in the (001)-oriented films and $g_{5g} \langle \epsilon_{5g}(z) \rangle$ and g_0 for the (111)-oriented film.

An upper limit for $\langle \epsilon_{3g\theta}(z) \rangle$ and $\langle \epsilon_{5g}(z) \rangle$ can be estimated knowing the normal stains $\epsilon_{3g\theta}$ and ϵ_{5g} , respectively. This enables one to evaluate lower limits for g_{3g} and g_{5g} . In estimation of g_{3g} we have used our experimental data on the 900-Å (001) film because it exhibits the maximum anisotropy in the g value; the lower limit for g_{5g} is obtained using films evaporated on quartz as sliding effects are not too important for these cases. Our estimations yield $g_{3g} > 0.5$ and $g_{5g} > 25.8$. Now, using Eqs. (7) and (8) as well as the wave functions given by Lea, Leask, and Wolf¹⁸ and the energy splitting between the Γ_7 ground state and the Γ_8 excited state given by Williams and Hirst¹⁹ or Follstaedt and Narath⁷ a lower limit for $G_{3g}^{(2)}$ and $G_{5g}^{(2)}$ can be estimated. We found for these orbit-lattice coupling parameters in Au:Yb the following lower limit:

$$G_{3g}^{(2)}/\alpha_J > 449 \text{ K}, \quad G_{5g}^{(2)}/\alpha_J > 650 \text{ K} \quad (15)$$

These values are of the order of magnitude of those found for Au:Er (Ref. 11) and also have the same magnitude as the second-order crystalline-field parameters found in hexagonal metals.²⁰

The point-charge model predicts the values of +1200 and +2400 K for the tetragonal second-order orbit-lattice coupling parameter, $G_{3g}^{(2)}/\alpha_J$ and the trigonal second-order orbit-lattice coupling parameter, $G_{5g}^{(2)}/\alpha_J$, respectively. Thus, the signs of $G_{3g}^{(2)}/\alpha_J$ and $G_{5g}^{(2)}/\alpha_J$ for Au:Yb are consistent with the prediction of the point-charge model. Also in a previous Au:Er (Refs. 9 and 12) thin-film experiment the sign of the tetragonal and trigonal orbit-lattice coupling constant agree with the prediction of the point-charge model. These observations are in contrast to the observation in Ag:Er (Ref. 10) and Ag:Dy (Ref. 11) thin films where the trigonal second-order orbit-lattice coupling constant was found to have opposite sign to that predicted by the point-charge model while the tetragonal orbit-lattice constant does agree with the point-charge model. These observations cannot

be explained by a d virtual bound state or p virtual bound state model. It should be stressed that the point-charge model cannot account for the sign of the fourth-order static cubic crystalline-field parameter of rare-earth gold dilute alloys and d virtual bound-state model was invoked to explain the sign of this parameter.¹⁹ According to the virtual bound-state model, the crystalline field of the ligands splits the $5d$ virtual bound state on the rare-earth site into $d\epsilon$ (xy , yz , zx symmetry) and $d\gamma$ ($3z^2 - r^2$, $x^2 - y^2$) levels, the $d\epsilon$ state being lower. Consequently, the sign of the crystalline field could be reversed due to the aspherical charge distribution associated with occupied $d\epsilon$ states.

Trigonal distortion cannot split the $d\epsilon$ virtual bound state and consequently if the splitting between $d\epsilon$ and $d\gamma$ levels is bigger than their widths, $5d$ screening electrons cannot contribute to the second-order trigonal orbit-lattice coupling parameter $G_{5g}^{(2)}$. This is also true for the case of p virtual state which remain unsplit under trigonal distortion. The situation is different, when a tetragonal distortion is applied. In this case the degeneracy of both $d\epsilon$ and the p virtual states are lifted leading to a doubly degenerate state and a single state. Consequently both p and d virtual bound states can contribute to $G_{3g}^{(2)}$. Experimentally, however, evidence exist for the failure of the point-charge model in all cases¹⁰⁻¹² when trigonal distortion was applied. This indicates that virtual d or p states do not play an important role in determining the sign and magnitude of the second-order orbit-lattice coupling constant in noble metals doped with rare-earth ions. The possibility for a f virtual state to be responsible for the failure of the point-charge model in trigonal Ag:Er and Ag:Dy thin films is very unlikely. Thus, the failure of the point-charge model in trigonal second-order orbit-lattice constant in Ag:Er and Ag:Dy is not understood yet.

The values of g_0 as found by our fitting procedure are tabulated in Table I. These values agree within the error bars with the g values found in strain-free films or even with the values observed previously in the bulk.¹ This yields an upper limit on a change of the g shift $\delta(\Delta g_{ce})$, either in expansion (quartz substrate) or compression (NaCl substrate), which is $|\delta(\Delta g_{ce})| < 0.015$. Using this value together with $|\Delta g_{ce}| \approx 0.08$, $|\delta V/V| \approx 0.01$ and Eq. (12) for the free-electron model, we can estimate the upper limit for $|\partial(\ln J)/\partial(\ln V)|$ to be of the order of 18.

In a series of ESR experiments down to 0.5 K on Au:Yb¹⁷⁰ and Au_{1-x}Ag_x:Yb¹⁷⁰ ($0 \leq x \leq 0.30$) powdered and single-crystal diluted alloys, we were not able to detect any anomaly in the g shift and thermal broadening, associated with a Kondo effect. These results were independent of any thermal treatment of the samples. This observation is in disagreement to that of Nagel *et al.*²¹ We believe that Yb³⁺ impurities tend to sit in Au clusters and consequently

the effect of Ag is not significant.

In summary, our measurements would support the conclusions of the nuclear orientation study⁶ and the magnetization study⁵ of Au:Yb that the Kondo temperature is indeed very low.

ACKNOWLEDGMENTS

This work was financially supported by CNPq and FAPESP, Brazil.

-
- *Permanent address: Phys. Dept., Hebrew University, Jerusalem, Israel.
- ¹L. J. Tao, D. Davidov, R. Orbach, and E. P. Chock, *Phys. Rev. B* **4**, 5 (1971); E. P. Chock, D. Davidov, R. Orbach, C. Rettori, and L. J. Tao, *ibid.* **5**, 2735 (1972).
- ²A. D. Murani, *Solid State Commun.* **12**, 295 (1973).
- ³F. Gonzalez-Jimenez and P. Imbert, *Solid State Commun.* **13**, 85 (1973).
- ⁴F. Gonzalez-Jimenez, B. Cornut, and B. Coqblin, *Phys. Rev. B* **11**, 4674 (1975).
- ⁵G. Frossati, J. M. Mignot, D. Thoulouze, and R. Tournier, *Phys. Rev. Lett.* **36**, 203 (1976).
- ⁶A. Benoit, J. Floquet, and J. Sanchez, *Phys. Rev. B* **9**, 1092 (1975).
- ⁷D. Follstaedt and A. Narath, *Phys. Rev.* **19**, 1374 (1949); *Phys. Rev. Lett.* **37**, 1490 (1976).
- ⁸D. Arbilly, G. Deutscher, E. Grumbaum, R. Orbach, and J. T. Suss, *Phys. Rev. B* **12**, 5068 (1975).
- ⁹J. F. Suassuna, G. E. Barberis, C. Rettori, and C. A. Pelá, *Solid State Commun.* **22**, 347 (1977).
- ¹⁰G. E. Barberis, J. F. Suassuna, C. Rettori, and C. A. Pelá, *Solid State Commun.* **23**, 603 (1977).
- ¹¹C. A. Pelá, G. E. Barberis, J. F. Suassuna, and C. Rettori, *Phys. Rev. B* **21**, 34 (1980).
- ¹²C. A. Pelá, J. F. Suassuna, G. F. Barberis, and C. Rettori, *Phys. Rev. B* (in press).
- ¹³*American Handbook of Physics*, 2nd ed. (McGraw-Hill, New York, 1973).
- ¹⁴J. S. Schilling, P. J. Ford, U. Larson, and J. A. Mydosh, *Phys. Rev. B* **14**, 4368 (1976).
- ¹⁵J. S. Schilling, *Adv. Phys.* **28**, 657 (1979), and references therein.
- ¹⁶M. Peter, D. Shaltiel, J. H. Wernick, H. J. Williams, J. B. Mock, and R. C. Sherwood, *Phys. Rev.* **126**, 1395 (1962).
- ¹⁷R. Calvo, S. B. Oseroff, C. Fainstein, H. C. G. Passeggi, and M. Tovar, *Phys. Rev. B* **9**, 4888 (1974).
- ¹⁸K. R. Lea, M. J. M. Leask, and W. P. Wolf, *J. Phys. Chem. Solids* **23**, 1381 (1962).
- ¹⁹G. Williams and L. L. Hirst, *Phys. Rev.* **185**, 407 (1969).
- ²⁰P. Touborg and J. Hog, *Phys. Rev. Lett.* **33**, 775 (1974); P. Touborg, R. Nevald, and J. Johansson, *Phys. Rev. B* **17**, 4454 (1978).
- ²¹J. Nagel, S. Hüfner, and M. Grünig, *Solid State Commun.* **13**, 1279 (1973).